Psychological Medicine

cambridge.org/psm

Individualized prediction of dispositional worry using white matter connectivity

Chunliang Feng[1,2,3,*], Zaixu Cui[2,4,*], Dazhi Cheng[5], Rui Xu[1] and Ruolei Gu[6,7]

[1]Institute of Basic Research in Clinical Medicine, China Academy of Chinese Medical Sciences, Beijing 100700, China; [2]State Key Laboratory of Cognitive Neuroscience and Learning, Beijing Normal University, Beijing 100875, China; [3]College of Information Science and Technology, Beijing Normal University, Beijing 100875, China; [4]Department of Psychiatry, Perelman School of Medicine, University of Pennsylvania, Philadelphia, PA19104, USA; [5]Department of Pediatric Neurology, Capital Institute of Pediatrics, Beijing 100020, China; [6]CAS Key Laboratory of Behavioral Science, Institute of Psychology, Beijing 100101, China and [7]Department of Psychology, University of Chinese Academy of Sciences, Beijing 100049, China

Abstract

Background. Excessive worry is a defining feature of generalized anxiety disorder and is present in a wide range of other psychiatric conditions. Therefore, individualized predictions of worry propensity could be highly relevant in clinical practice, with respect to the assessment of worry symptom severity at the individual level.

Methods. We applied a multivariate machine learning approach to predict dispositional worry based on microstructural integrity of white matter (WM) tracts.

Results. We demonstrated that the machine learning model was able to decode individual dispositional worry scores from microstructural properties in widely distributed WM tracts (mean absolute error = 10.46, $p < 0.001$; root mean squared error = 12.82, $p < 0.001$; prediction $R^2 = 0.17$, $p < 0.001$). WM tracts that contributed to worry prediction included the posterior limb of internal capsule, anterior corona radiate, and cerebral peduncle, as well as the corticolimbic pathways (e.g. uncinate fasciculus, cingulum, and fornix) already known to be critical for emotion processing and regulation.

Conclusions. The current work thus elucidates potential neuromarkers for clinical assessment of worry symptoms across a wide range of psychiatric disorders. In addition, the identification of widely distributed pathways underlying worry propensity serves to better improve the understanding of the neurobiological mechanisms associated with worry.

Introduction

Worry is defined as a chain of thoughts and images that are negatively affect-laden, emerging when one anticipates a potential threat, but doubts his/her ability to cope (Borkovec *et al.*, 1998; Brosschot *et al.*, 2006). Although emotionally disturbing, previous studies suggest that worry has its adaptive functions and could be considered a compensatory strategy employed in response to perceived danger (Newman *et al.*, 2013). However, worry can become chronic and intolerable if not effectively regulated, which results in discomfort, disruption, and a decline in quality of life (Borkovec *et al.*, 1998). Indeed, worry constitutes an important transdiagnostic process that pervades many anxiety and mood disorders (Ehring and Watkins, 2008; Sharp *et al.*, 2015; Barlow *et al.*, 2016). For instance, the central feature of generalized anxiety disorder (GAD) is chronic, excessive, and uncontrollable worry (Borkovec and Inz, 1990; Borkovec *et al.*, 2004). Likewise, worry has frequently been associated with major depression (Chelminski and Zimmerman, 2003) and neuroticism (Servaas *et al.*, 2014).

Taken together, worry is a pervasive experience in humans, and yet, individuals exhibit wide heterogeneity in their propensity to experience worrisome thoughts. Therefore, establishing predictive models to assess current worry symptoms would have potential clinical value. In the current study, we aimed to decode dispositional worry from neuroimaging data. Our purpose was to establish potential neural markers that are indicative of worry as a core symptom of psychiatric disorders.

Previous neuroimaging studies revealed the correlation of worry propensity with activity and structural changes in emotion processing (e.g. amygdala) and regulation (e.g. prefrontal cortex) regions. Also shown previously, is the correlation of worry propensity with functional and structural connectivity between these neural networks. Stronger worry tendencies were associated with lower activation in response to aversive events in the prefrontal cortex and anterior cingulate cortex (ACC) (Schienle *et al.*, 2009), as well as lower ACC and prefrontal cortex volumes, and higher striatal volume (Hilbert *et al.*, 2015; Andreescu *et al.*, 2017). Furthermore, functional couplings between prefrontal and limbic regions account for worry tendencies, such that higher dispositional worry is correlated with weaker functional connectivity in the prefrontal–limbic pathway (Makovac *et al.*, 2016; Meeten *et al.*, 2016). Lastly,

Original Article

*These authors contributed equally to this work.

Cite this article: Feng C, Cui Z, Cheng D, Xu R, Gu R (2019). Individualized prediction of dispositional worry using white matter connectivity. *Psychological Medicine* **49**, 1999–2008. https://doi.org/10.1017/S0033291718002763

Received: 19 December 2017
Revised: 12 June 2018
Accepted: 29 August 2018
First published online: 25 October 2018

Key words:
Cross-validation; diffusion tensor imaging; machine learning; relevance vector regression; worry

Author for correspondence:
Rui Xu, Ruolei Gu, E-mail: xvr@cacms.cn, gurl@psych.ac.cn

© Cambridge University Press 2018

CAMBRIDGE UNIVERSITY PRESS

evidence derived from diffusion tensor imaging (DTI) research has indicated that worry propensity is related to white matter (WM) integrity in the frontal cortex, ACC, and amygdala (Zhang *et al.*, 2013a, b; Andreescu *et al.*, 2017). In particular, higher worry severity was associated with decreased mean diffusivity (MD) in the left orbital frontal cortex and ACC, as well as increased MD in the right putamen (Andreescu *et al.*, 2017), and increased fractional anisotropy (FA) in the amygdala (Zhang *et al.*, 2013a, b). Furthermore, previous DTI studies revealed that GAD is associated with lower FA in the uncinate fasciculus, a primary WM tract connecting the amygdala and frontal cortex (Ayling *et al.*, 2012; Hettema *et al.*, 2012; Tromp *et al.*, 2012; Liao *et al.*, 2014). Additionally, compared with controls, GAD patients also exhibited reduced FA in the inferior fronto-occipital fasciculus, inferior longitudinal fasciculus, and corona radiate (Liao *et al.*, 2014). Besides previous studies on dispositional worry or GAD, there is also evidence showing that mood and anxiety disorder is associated with WM integrity in other tracts implicated in emotional processing, including fornix and cingulum (Abe *et al.*, 2006; Yu *et al.*, 2017). Taken together, previous findings suggest that mood and anxiety disorder is closely associated with interactions between networks responsible for emotion regulation and processing (e.g. prefrontal and limbic networks), and thus provide potential candidates for the neuromarkers of trait worry.

Importantly however, previous findings on the neural basis of dispositional worry were based on the univariate correlational approach, which is subject to several serious limitations. First, univariate analysis possesses limited sensitivity to identify subtle and spatially distributed effects. Subtle and distributed information across large-scale neural networks might play a critical role in maintaining worry tendencies. This is especially pertinent considering that worry is a multi-faceted construct, and presumably relies on the functional and structural integrity of distributed networks. In agreement with this assertion, previous studies using the univariate approach often reported inconsistent findings on the neural substrates of worry propensity (Paulesu *et al.*, 2010; Zhang *et al.*, 2011; Liao *et al.*, 2014; Bergamino *et al.*, 2017). Second, the traditional in-sample correlation approach is prone to overfitting, and the correlational results do not always allow for out-of-sample generalizations (Gabrieli *et al.*, 2015; Dubois and Adolphs, 2016; Yarkoni and Westfall, 2017). In this case, previous correlational findings are not readily applicable to clinical practice, where doctors require individualized assessment of symptom severity (Paulus, 2015, 2017; Huys *et al.*, 2016). To address these issues, we implemented a multivariate pattern analysis (MVPA) approach to identify DTI features that are predictive of current dispositional worry at the individual level.

In particular, the current approach provides the following advantages. First, the multivariate nature of the analysis enables the detection of subtle and spatially distributed effects. MVPA approaches are particularly suitable for examining neural mechanisms underlying complex traits such as dispositional worry and relevant mental disorders (e.g. GAD), thought to be rooted in disturbed functional and structural integrity of distributed networks (Etkin *et al.*, 2009; Hilbert *et al.*, 2014). In line with this conjecture, a recent review proposed that machine learning algorithms and multivariate tools could be eminently useful for characterizing neuroanatomy of GAD (Fonzo and Etkin, 2017). Second, the machine learning approach allows for the prediction of unseen participants, offering information at the individual level rather than group level. More specifically, the machine learning approach typically implements cross-validation procedures to estimate the model with training samples, and to test the model performance with independent samples (i.e. test samples). As such, the current work aimed to identify brain measures, i.e. WM connectivity, that are predictive of current worry symptoms at the individual level, rather than to predict future worry symptoms. Moreover, discriminating features adopted by the model can be employed as neuroimaging markers for worry tendencies.

In light of previous studies on worry symptoms and WM integrity (Zhang *et al.*, 2013a, b; Andreescu *et al.*, 2017; Bergamino *et al.*, 2017), we hypothesized that dispositional worry scores would be predicted by structural integrity within the emotion processing and regulation neural network, particularly the prefrontal cortex, ACC, and amygdala. Moreover, based on previous DTI studies on mood and anxiety disorders (Hettema *et al.*, 2012; Tromp *et al.*, 2012; Liao *et al.*, 2014), we further hypothesized that WM tracts, including the uncinate fasciculus, inferior fronto-occipital fasciculus, inferior longitudinal fasciculus, cingulum, fornix, and corona radiate, would contribute to the prediction of current trait worry.

Material and methods

Participants

Fifty-nine adult participants (35 females; age 26.19 ± 7.13 years, range: 18–49 years) were recruited. All the participants were right handed, had received junior high school or above education, and used Chinese as their first language. All were clear of organic brain diseases or any abnormal nervous system manifestations. The study was conducted in accordance with the 1964 Declaration of Helsinki and its later amendments, and was approved by the Ethics Committee of Beijing Normal University. Written informed consent was obtained from all participants.

Penn State Worry Questionnaire

To assess individual dispositional worry, we administered the Chinese version of the Penn State Worry Questionnaire (PSWQ) (Meyer *et al.*, 1990), which measures general tendency toward frequent and excessive worry in both clinical and non-clinical samples. The PSWQ consists of 16 items; each item is scored on a five-point Likert scale ranging from 1 (not at all typical) to 5 (very typical). The reliability and validity of the PSWQ have been demonstrated by previous studies (Meyer *et al.*, 1990; Brown *et al.*, 1992).

MRI data acquisition

Images were acquired with a Siemens TRIO 3-Tesla scanner at the Beijing Normal University Imaging Center for Brain Research. High-resolution structural images were acquired through a 3D sagittal T1-weighted magnetization-prepared rapid acquisition with gradient-echo sequence, using the following parameters: sagittal slices, 144; TR, 2530 ms; TE, 3.39 ms; slice thickness, 1.33 mm; voxel size, 1 mm × 1 mm × 1.33 mm; flip angle, 7°; inversion time, 1100 ms; FOV, 256 mm × 256 mm. In addition, for DTI scans, a single-shot, twice-refocused spin-echo diffusion echo-planar imaging sequence was applied with the following parameters: TR, 8000 ms; TE, 89 mm; 30 optimal diffusion-weighted directions with a *b*-value of 1000 s/mm^2 and one

https://doi.org/10.1017/S0033291718002763 Published online by Cambridge University Press

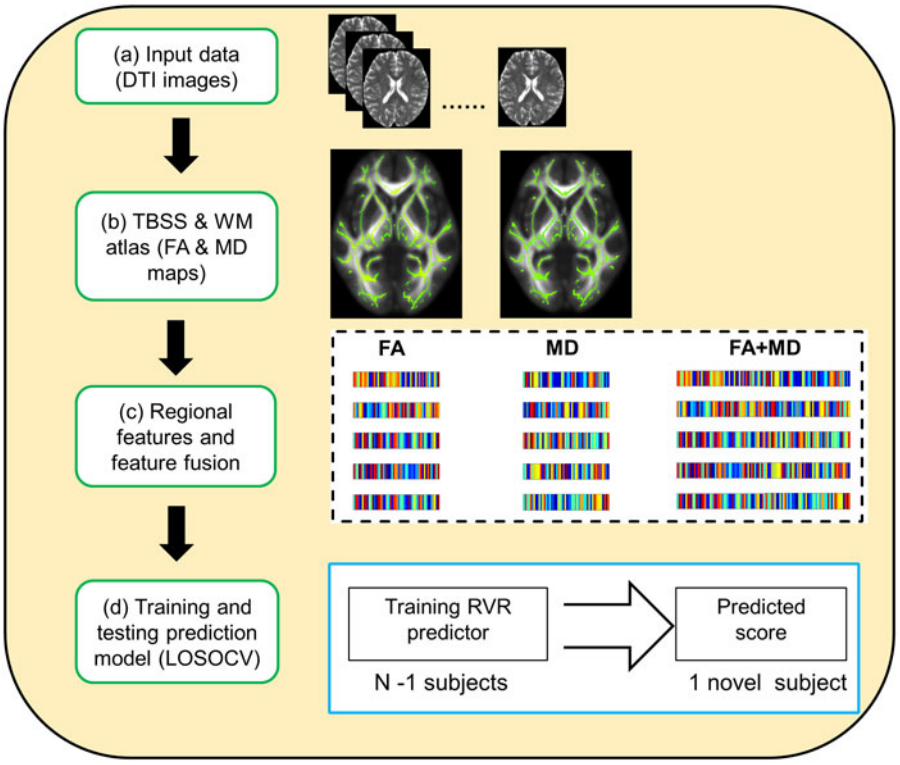


Fig. 1. Schematic overview of the prediction framework. DTI, diffusion tensor imaging; TBSS, tract-based spatial statistics; WM, white matter; FA, fractional anisotropy; MD, mean diffusivity; LOSOCV, leave-one-subject-out cross-validation.

image with a *b*-value of 0 s/mm^2; data matrix, 128 × 128; FOV, 282 mm × 282 mm; slice thickness, 2.2 mm; 62 axial slices with no interslice gap; voxel size, 2.2 mm × 2.2 mm × 2.2 mm. To increase the signal-to-noise ratio, two repetitions were performed, with a total imaging time of 12 min.

Image preprocessing

Processing of the diffusion MRI dataset was implemented using PANDA (http://www.nitrc.org/projects/panda), which is a pipeline toolbox for diffusion MRI analysis (Cui *et al.*, 2013) based on FSL (Jenkinson *et al.*, 2012). The procedure included skull-stripping, simple-motion and eddy-current correction, and diffusion tensor/parameter calculation. The following two diffusion metrics were calculated: (i) FA, a measure of the fraction of the magnitude of the tensor that can be attributed to the anisotropic diffusion (Basser, 1995); (ii) MD, a measure of average diffusion across different directions (Basser *et al.*, 1994). FA and MD are the most commonly used diffusion parameters, and are thought to provide complementary information about diffusion (Beaulieu, 2002; Alexander *et al.*, 2011). Tract-based spatial statistics was employed to extract the core (skeleton) of WM (Smith *et al.*, 2006). In detail, all FA images were registered to the template, and then averaged to generate a mean FA image. The FA skeleton, which represented the core tracts that were common to all subjects, was calculated using the mean FA. This skeleton was then thresholded (FA value >0.2) to further remove non-WM regions. Each individual subject's registered FA and MD images were projected to this skeleton, and FA and MD skeleton images were produced for each subject. Following this, we calculated the regional average FA and MD skeleton using the WM Parcellation Map (WMPM), which is a prior WM atlas defined in the MNI space with 50 'core WM' regions (Mori *et al.*, 2008). As each subject's FA/MD skeleton and the WMPM atlas were both in MNI space and both with a resolution of 1 mm × 1 mm × 1 mm, we overlaid the skeleton images on the atlas to categorize each skeleton voxel into the 50 WM regions (Huang *et al.*, 2011; Tseng *et al.*, 2013). For each participant, the mean FA and MD skeletons were acquired for each of the 50 WM regions.

Multivariate relevance vector regression analysis

The average FA and MD values for the 50 regions were concatenated to yield a feature vector for each subject (Cui *et al.*, 2016). The feature vector therefore consisted of 50 FA features and 50 MD features. The use of different types of features together in the model likely improves prediction performance, since distinct features putatively capture complementary aspects of WM tissue (Alexander *et al.*, 2011). Indeed, previous studies indicate that using FA and MD features together resulted in higher model performance than using each type of features alone (Ross and Jain, 2003; Damoiseaux and Greicius, 2009; Wee *et al.*, 2011; Dai *et al.*, 2012; Xie *et al.*, 2015; Cui *et al.*, 2016).

The relationship between PSWQ scores and microstructural WM properties was examined using multivariate relevance vector regression (RVR) with a linear kernel as implemented in PRoNTo (http://www.mlnl.cs.ucl.ac.uk/pronto/) and in-house scripts running under Matlab environment (Mathworks, 2016 release) (Fig. 1). RVR is a sparse kernel learning multivariate regression method set in a fully probabilistic Bayesian framework (Tipping, 2001). In this framework, a zero-mean Gaussian prior is introduced over the model weights, and is governed by a set of hyper-parameters, one for each weight. The most probable values for these hyper-parameters are then iteratively estimated from the training data, with sparseness achieved due to posterior

https://doi.org/10.1017/S0033291718002763 Published online by Cambridge University Press

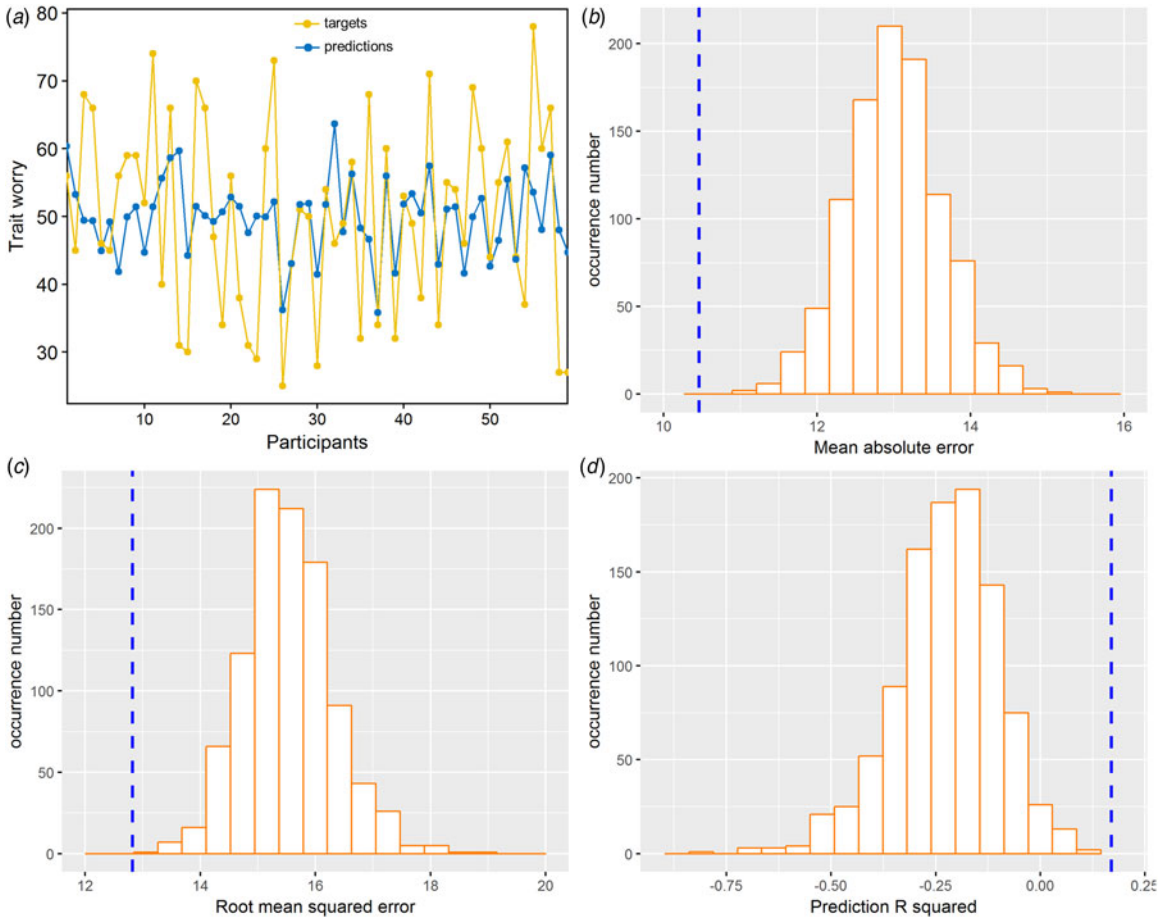


Fig. 2. RVR findings of the multivariate regression analysis in dispositional worry prediction using leave-one-subject-out cross-validation procedures. (*a*) Line plot showing consistency between actual and predicted dispositional worry scores. (*b*) Distribution of permutation of the mean absolute error. (*c*) Distribution of permutation of the root mean squared error. (*d*) Distribution of permutation of the prediction R^2. The values obtained using real scores are indicated by the blue dashed line.

Table 1. Results of RVR prediction using combined WM features or a single WM feature

	LOSOCV			10-fold CV		
Feature	MAE	RMSE	Prediction R^2	MAE	RMSE	Prediction R^2
Combined	10.46	12.82	0.17	10.68	13.65	0.055
FA	11.47	14.48	−0.06	11.88	14.79	−0.11
MD	11.85	14.15	−0.01	12.01	14.3	−0.037

LOSOCV, leave-one-subject-out cross-validation; FA, fractional anisotropy; MD, mean diffusivity; MAE, mean absolute error; RMSE, root mean squared error.

distributions of many of the weights peaking sharply around zero. Those training vectors associated with non-zero weights are referred to as 'relevance' vectors. The optimized posterior distribution of the weights can then be used to predict the target value (e.g. anxiety score) for a previously unseen feature vector, by computing the predictive distribution (Tipping, 2001).

In the current work, a leave-one-subject-out cross-validation (LOSOCV) was used to evaluate the out-of-sample prediction performance. *N*-1 subjects (where *N* is the number of subjects) were used as the training set, with the remaining individual used as the testing sample. During the training procedure, each feature was linearly scaled to a range of zero to one across the training set, and then a RVR prediction model was constructed using this training set. During the testing procedure, each testing subject's feature vector was scaled using the scaling parameter acquired during the training procedure. Following this, the RVR prediction model was used to predict the testing subjects' PSWQ score (Gong *et al.*, 2014; Cui et al., 2018). The training and testing procedures were repeated *N* times such that each subject was used once as the testing subject.

The accuracy of prediction was measured with three frequently used statistics (Franke *et al.*, 2010; Gong *et al.*, 2014; Cui et al., 2018): (i) mean absolute error (MAE): $\frac{1}{n}\sum_{i=1}^{n}|y_i-\hat{y}_i|$; (ii) root mean squared error (RMSE): $\sqrt{\frac{1}{n}\sum_{i=1}^{n}(y_i-\hat{y}_i)^2}$; (iii) *prediction* R^2: $1-\frac{\sum_{i=1}^{n}(y_i-\hat{y}_i)^2}{\sum_{i=1}^{n}(y_i-\bar{y})^2}$. Please note that n indicates sample size, y_i indicates

https://doi.org/10.1017/S0033291718002763 Published online by Cambridge University Press

Table 2. Contributing white matter connectivity features with an absolute weight score higher than 30% of the maximum absolute weight value for RVR to predict dispositional worry

WM labels	Metric	Weight score
FA features		
Posterior limb of internal capsule (L)	FA	0.293
Anterior corona radiata (L)	FA	0.176
Cingulum (cingulate part) (R)	FA	0.176
Inferior fronto-occipital fasciculus (L)	FA	0.174
Genu of corpus callosum	FA	0.162
Anterior corona radiata (R)	FA	0.159
Superior cerebellar peduncle (R)	FA	0.157
Sagittal stratum (R)	FA	0.144
Uncinate fasciculus (L)	FA	0.133
Retrolenticular part of internal capsule (R)	FA	0.122
Posterior limb of internal capsule (R)	FA	0.119
Corticospinal tract (L)	FA	0.106
Superior cerebellar peduncle (L)	FA	0.103
Pontine crossing tract	FA	0.101
Inferior cerebellar peduncle (R)	FA	0.099
Superior fronto-occipital fasciculus (L)	FA	0.099
Cerebral peduncle (L)	FA	0.088
MD features		
Cerebral peduncle (R)	MD	0.246
Fornix (cres)/stria terminalis (L)	MD	0.243
Cerebral peduncle (L)	MD	0.233
Inferior cerebellar peduncle (L)	MD	0.203
Inferior fronto-occipital fasciculus (L)	MD	0.183
Tapetum (L)	MD	0.182
Genu of corpus callosum	MD	0.180
Uncinate fasciculus (L)	MD	0.153
Posterior limb of internal capsule (R)	MD	0.146
Posterior thalamic radiation (L)	MD	0.137
Superior cerebellar peduncle (L)	MD	0.133
Cingulum (cingulate part) (L)	MD	0.130
Body of fornix	MD	0.124
Superior fronto-occipital fasciculus (L)	MD	0.123
Posterior thalamic radiation (R)	MD	0.102
Splenium of corpus callosum	MD	0.089
Anterior corona radiata (L)	MD	0.089
Superior corona radiata (L)	MD	0.086

WM, white matter; L, left; R, right; FA, fractional anisotropy; MD, mean diffusivity.

actual worry score of the i^{th} subject, $\hat{y}_i$ indicates predicted worry score of the i^{th} subject, and $\bar{y}$ indicates mean of the actual worry scores across all subjects. The permutation test was applied to determine whether the obtained metrics were significantly better than those expected by chance. More specially, we permuted PSWQ scores across training samples without replacement 1000 times, and each time re-applied the above LOSOCV prediction procedure. The permutation resulted in a distribution of MAE, RMSE, and *prediction* R^2 values reflecting the null hypothesis that the model did not exceed chance level. The number of times that the permuted value was greater than (or, with respect to MAE and RMSE values, less than) the true value, was then divided by 1000, providing an estimated p value for each statistic.

Contributing features and corresponding weights

To quantify the contribution of each feature to prediction, we constructed a new RVR model using all subjects. The absolute value of the RVR weight of each feature quantifies its contribution to the model (Gong *et al.*, 2014; Cui and Gong, 2018; Cui et al., 2018). Please note that RVR calculates the weight for samples. As RVR is a sparse model in the sample space, most weight will be zero; remaining samples with non-zero weight were used to fit the model. The regression coefficients of all features were determined as the weighted sum of the feature vector of the non-zero weighted samples (see also Gong *et al.*, 2014; Cui and Gong, 2018). A larger absolute value of weight indicates a greater contribution of the corresponding feature to prediction, in the context of every other feature (Gong *et al.*, 2014; Erus *et al.*, 2015; Cui and Gong, 2018; Cui et al., 2018). The feature was selected for visualization if the absolute value of its weight was higher than 30% of the maximum absolute weight value across features (i.e. 0.293, observed on the left posterior limb of internal capsule); this was consistent with previous studies (Ecker *et al.*, 2010; Gong *et al.*, 2014). We applied this threshold to eliminate noise components for a better visualization of the most discriminating regions (Ecker *et al.*, 2010; Gong *et al.*, 2014).

Validation

A 10-fold cross-validation was applied to validate our prediction results. All subjects were divided into 10 subsets, in which nine were used as the training set, and the remaining one was used as the testing set. The training set was scaled and used to train a RVR prediction model, which was then used to predict the scores for the scaled testing data. The scaling of testing data used parameters acquired from training data. This procedure was repeated 10 times, so that each subset was used as testing set once. Finally, the correlation r and MAE between the true and predicted scores were calculated across all subjects. Since the full dataset was randomly divided into 10 subsets, performance might have depended on data division. Therefore, the 10-fold cross-validation was repeated 100 times, and the results were averaged to produce a final prediction performance. A permutation test was applied 1000 times to test the significance of the prediction performance.

Results

Multivariate RVR analysis

The application of RVR to the combined FA and MD features allowed individualized prediction of PSWQ scores (MAE = 10.46, $p < 0.001$; RMSE = 12.82, $p < 0.001$; *prediction* $R^2 = 0.17$, $p < 0.001$; Fig. 2). Prediction performance worsened when using the single-type metric (FA or MD) (Table 1). The permutation test revealed a higher correlation coefficient and lower MAE

https://doi.org/10.1017/S0033291718002763 Published online by Cambridge University Press



Fig. 3. Contributing white matter connectivity features with an absolute weight score higher than 30% of the maximum absolute weight value for RVR to predict dispositional worry. (*a*) FA features. (*b*) MD features.

for the combined features, as compared with the FA or MD feature alone (combined *v.* FA: $p_{MAE} = 0.029$, $p_{RMSE} = 0.014$, $p^2_{prediction\ R} = 0.019$; combined *v.* MD: $p_{MAE} = 0.011$, $p_{RMSE} = 0.027$, $p^2_{prediction\ R} = 0.039$).

Contributing WM features

Thirty-five WM features were selected, including 17 FA features and 18 MD features (Table 2 and Fig. 3). The 17 FA features were derived from the following WM regions (Fig. 3*a*): bilateral genu of corpus callosum, posterior limbic of internal capsule, anterior corona radiata, superior cerebellar peduncle, and pontine crossing tract; left inferior fronto-occipital fasciculus, left uncinate fasciculus, left superior fronto-occipital fasciculus, and left cerebral peduncle; right cingulum, right sagittal stratum, right retrolenticular part of internal capsule, and right inferior cerebellar peduncle. The 18 MD features were derived from the following WM regions (Fig. 3*b*): bilateral genu of corpus callosum, splenium of corpus callosum, and body of fornix; left fornix/stria terminalis, left cerebral peduncle, left inferior cerebellar peduncle, left cingulum, left superior corona radiata, left cerebral peduncle, left inferior fronto-occipital fasciculus, left tapetum, left uncinate fasciculus, left posterior thalamic radiation, left superior cerebellar peduncle, left cingulum, left superior fronto-occipital fasciculus, left anterior and superior corona radiate; right posterior thalamic radiation, right cerebral peduncle, and right posterior limb of internal capsule.

Validation

The 10-fold cross-validation was used to re-estimate the performance of prediction. The resultant correlation coefficient and MAE values remained significant (MAE = 11.09, $p < 0.005$; RMSE = 13.65, $p < 0.005$; *prediction* $R^2 = 0.055$, $p < 0.005$; Fig. 4), thus validating the main findings derived from the LOSOCV approach.

Discussion

Excessive worry is a defining feature of GAD, and contributes to a wide range of other psychiatric disorders (Ehring and Watkins, 2008; Sharp *et al.*, 2015; Barlow *et al.*, 2016). However, the neurobiological markers of worry propensity remain largely unknown. In the current study, we employed WM microintegrity in a machine learning framework to make continuously valued predictions on dispositional worry. Our aim was to establish neuromarkers that are predictive of worry propensity at the individual level. We demonstrated that multivariate patterns of WM structural connectivity extracted from DTI data were sufficient to decode individual worry tendencies. In particular, inter-individual variation in trait worry was predicted by microstructural properties of widely distributed WM tracts. These tracts included the posterior limb of internal capsule, anterior corona radiate, and cerebral peduncle, as well as the corticolimbic pathways (e.g. uncinate fasciculus, cingulum, and fornix) already known to be critical for emotion processing and regulation.

It has been hypothesized that the neural pathways associated with emotion processing and regulation play a critical role in developing and maintaining chronic/dispositional worry and GAD (Etkin *et al.*, 2009; Schienle *et al.*, 2009; Etkin *et al.*, 2010; Makovac *et al.*, 2016; Meeten *et al.*, 2016). This is in line with our findings that WM tracts in the prefrontal–limbic pathway contribute to the predictions of worry propensity. For instance, the uncinate fasciculus is the primary WM tract that connects the ventral regions of the prefrontal cortex and ACC to the amygdala and other limbic regions (Ghashghaei *et al.*, 2007). Disrupted integrity of the uncinate fasciculus has been reliably identified in anxiety and depression disorders (Kim and Whalen, 2009; Phan

https://doi.org/10.1017/S0033291718002763 Published online by Cambridge University Press

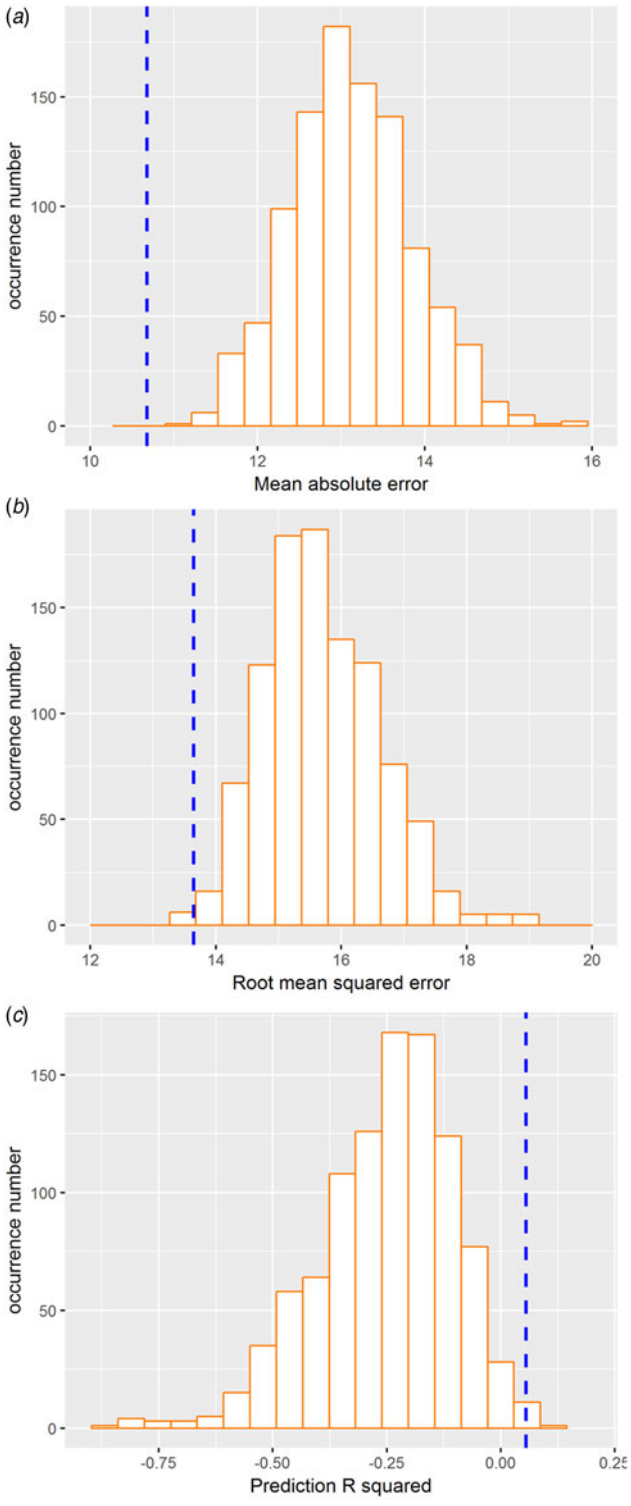


Fig. 4. RVR findings of the validation analysis using 10-fold cross-validation procedures. (*a*) Distribution of permutation of the mean absolute error. (*b*) Distribution of permutation of the root mean squared error. (*c*) Distribution of permutation of the prediction R^2. The values obtained using real scores are indicated by the blue dashed line.

et al., 2009; Ayling *et al.*, 2012; Carballedo *et al.*, 2012; Hettema *et al.*, 2012; Tromp *et al.*, 2012). Furthermore, integrity of the uncinate fasciculus predicts the functional connectivity strength of prefrontal regions and the amygdala (Tromp *et al.*, 2012), which has been associated with trait worry scores and emotion regulation ability (Makovac *et al.*, 2016). The cingulum bundle is the most prominent WM tract in the limbic system, and connects the ACC to the amygdala and hippocampus. Previous studies have revealed altered cingulum bundle integrity in post-traumatic stress disorder, and found the correlation between cingulum integrity and symptom severity (Abe *et al.*, 2006; Kim *et al.*, 2006). The fornix is a fiber tract originating from hippocampus and projecting to the hypothalamus and cingulate cortex among other regions (Saunders and Aggleton, 2007). As an important part of the Papez circuit in the limbic system, the fornix is thought to contribute to emotion regulation through higher order frontal regions (Dalgleish, 2004). In accordance with this, WM tract integrity in the fornix has been related to trait anxiety, depression, harm avoidance, and early trauma experiences (Kazlouski *et al.*, 2011; Modi *et al.*, 2013; Hoogenboom *et al.*, 2014; Yu *et al.*, 2017).

Notably, WM tracts in the prefrontal–limbic pathway are not the only features contributing to the predictive model. Instead, the current approach demonstrated the involvement of widely distributed WM tracts, in line with the multi-faceted nature of worry. Specifically, we revealed the following fiber tracts as potential neuromarkers of dispositional worry: the inferior fronto-occipital fasciculus, posterior thalamic radiation, corpus callosum, and those in the motor system (e.g. corona radiata, internal capsule, cerebellar peduncle, cerebral peduncle, and pontine crossing tract).

The microstructure of the inferior fronto-occipital fasciculus has been linked to obsessive–compulsive disorder, depression, and anxiety-related personality traits (Bae *et al.*, 2006; Garibotto *et al.*, 2010; Westlye *et al.*, 2011). This WM tract has been considered a 'multi-function' bundle that subserves semantic and emotional processing among other functions (Martino *et al.*, 2010; Sarubbo *et al.*, 2013). These putative functions fit well with the abstract, verbal-linguistic, and valenced nature of worry (Borkovec *et al.*, 2004; Sibrava and Borkovec, 2006). Moreover, disrupted integrity of the posterior thalamic radiation and corpus callosum has been consistently identified in depression disorders (Liao *et al.*, 2013; Sarıçiçek *et al.*, 2016; Hermesdorf *et al.*, 2017), suggesting the importance of these tracts in emotion processing. Finally, abnormalities of WM connectivity in the motor system have frequently been reported in a wide range of psychiatric disorders, including depression (Bae *et al.*, 2006; Shen *et al.*, 2017) and anxiety (Westlye *et al.*, 2011; Zhang *et al.*, 2011; Liao *et al.*, 2014). In particular, the fiber tracts in the corona radiata and internal capsule of the motor system wire the cortex and thalamus (Goh *et al.*, 2011), and are critical in filtering sensory information and regulating emotions (Herrero *et al.*, 2002). Furthermore, an increasing body of empirical evidence has indicated the involvement of the cerebellum in emotion processing and regulation (Schutter and Van Honk, 2005), such that integrity of cerebellar fiber tracts has been linked to emotion processing ability (Peng *et al.*, 2013; Laricchiuta *et al.*, 2015). Taken together, these WM tracts might contribute to different aspects of emotion appraisal and regulation that are related to dispositional worry.

Interestingly, the current results reveal that WM features that are predictive of PSWQ scores are predominantly located in the left hemisphere. Many other studies have also found left hemisphere asymmetry to be associated with worry, in both resting state and during tasks (Hoehn-Saric *et al.*, 2004, 2005; Mohlman *et al.*, 2009). For instance, Mohlman *et al.* (2009) found a strong correlation between the activation of the left medial orbitofrontal cortex and worry scores among GAD patients.

https://doi.org/10.1017/S0033291718002763 Published online by Cambridge University Press

Also, Hoehn-Saric *et al.* (2004) reported that after clinical treatment using citalopram, GAD patients showed a reduction of brain activation, mostly in the left hemisphere, in response to experimental stimuli. To explain this pattern of asymmetry, Hoehn-Saric *et al.* (2005) pointed out that worry is a thought process that is primarily verbal-semantic. Therefore, the involvement of verbal thought activity might be more predominately associated with left hemisphere activation. That being said, it should be noted that the current evidence on the worry and hemisphere asymmetry is rather preliminary, and future studies are needed to address the issue.

Several limitations and future directions should be noted in relation to this study. First, our prediction was obtained from a relatively small subclinical sample. Therefore, generalization of the current findings requires further validation using a larger independent sample and other cross-validation methods. Second, although our results indicated that the performance of our model was significantly better than chance level, the MAE and RMSE scores were relatively large and the prediction R^2 score was moderate. Therefore, future studies are needed to improve the performance of the model by combining data from different levels of measure (e.g. behavioral and brain measures), different modalities (e.g. functional and structural connectivity), and different statistics (e.g. mean and variance). For instance, the current study employed the mean values of FA and MD from each fiber tract as features, since these metrics are known to reflect structural integrity (Assaf and Pasternak, 2008; Khong *et al.*, 2016; Martin *et al.*, 2016). However, other measures, such as the variance of these metrics within each tract might also be biologically meaningful, and could be explored in future studies. Nevertheless, the model proposed in the present study serves as a starting point, and should inspire further investigation to improve prediction accuracy and generalizability. On a related note, predicted scores exhibited smaller variance than the actual scores, which could be attributed to regression prediction models shrinking estimates toward the mean, as well as the fact that the current predictive model based on WM integrity did not fit perfectly with the actual worry scores (for additional observation and discussion on this issue, see also Rowen *et al.*, 2009; Brazier *et al.*, 2010; Versteegh *et al.*, 2010; Fayers and Hays, 2014). Finally, future clinical research should also examine whether the effectiveness of treatments used to reduce worry (e.g. cognitive behavior therapy; see Querstret and Cropley, 2013 for a review) could be affected by the individual differences in structural networks revealed in this study.

Despite these limitations, we here demonstrate that integrity of widely distributed WM tracts effectively predict dispositional worry at individual level. As such, the current work provides potential neuromarkers for clinical assessment of worry symptoms across a wide range of psychiatric disorders. In addition to the potential clinical applications, the current multivariate approach compared with previous mass-univariate techniques revealed more distributed pathways underlying worry propensity. Thus, these move us toward a better understanding of the neurobiological mechanisms of worry.

Acknowledgement. The authors thank two anonymous reviewers for their comments, which have helped improve the quality of the manuscript.

Author contributions. CF and RX designed the study. CF and RX performed the experiment. CF and ZC analyzed the data. CF, RX, ZC, and RG wrote the manuscript. DC provided suggestions on the revision of manuscript.

Financial support. This study was funded by the National Natural Science Foundation of China (81503480, 31571124, 31500920, 31700977), the Major Program of Chinese National Social Science Foundation (17ZDA324), the National Postdoctoral Program for Innovative Talents (BX201600019), the China Postdoctoral Science Foundation (2017M610055), the Beijing National Science Foundation (7154227), the Project of Institute of Basic Research in Clinical Medicine, and the China Academy of Chinese Medical Sciences (Z0414).

Conflict of interest. None.

References

Abe O, Yamasue H, Kasai K, Yamada H, Aoki S, Iwanami A, Ohtani T, Masutani Y, Kato N and Ohtomo K (2006) Voxel-based diffusion tensor analysis reveals aberrant anterior cingulum integrity in posttraumatic stress disorder due to terrorism. *Psychiatry Research: Neuroimaging* **146**, 231–242.

Alexander AL, Hurley SA, Samsonov AA, Adluru N, Hosseinbor AP, Mossahebi P, Tromp DP, Zakszewski E and Field AS (2011) Characterization of cerebral white matter properties using quantitative magnetic resonance imaging stains. *Brain Connectivity* **1**, 423–446.

Andreescu C, Tudorascu D, Sheu LK, Rangarajan A, Butters MA, Walker S, Berta R, Desmidt T and Aizenstein H (2017) Brain structural changes in late-life generalized anxiety disorder. *Psychiatry Research: Neuroimaging* **268**, 15–21.

Assaf Y and Pasternak O (2008) Diffusion tensor imaging (DTI)-based white matter mapping in brain research: a review. *Journal of Molecular Neuroscience* **34**, 51–61.

Ayling E, Aghajani M, Fouche J-P and van der Wee N (2012) Diffusion tensor imaging in anxiety disorders. *Current Psychiatry Reports* **14**, 197–202.

Bae JN, MacFall JR, Krishnan KRR, Payne ME, Steffens DC and Taylor WD (2006) Dorsolateral prefrontal cortex and anterior cingulate cortex white matter alterations in late-life depression. *Biological Psychiatry* **60**, 1356–1363.

Barlow DH, Allen LB and Choate ML (2016) Toward a unified treatment for emotional disorders – republished article. *Behavior Therapy* **47**, 838–853.

Basser PJ (1995) Inferring microstructural features and the physiological state of tissues from diffusion-weighted images. *NMR in Biomedicine* **8**, 333–344.

Basser PJ, Mattiello J and LeBihan D (1994) Estimation of the effective self-diffusion tensor from the NMR spin echo. *Journal of Magnetic Resonance, Series B* **103**, 247–254.

Beaulieu C (2002) The basis of anisotropic water diffusion in the nervous system – a technical review. *NMR in Biomedicine* **15**, 435–455.

Bergamino M, Farmer M, Yeh H-W, Paul E and Hamilton JP (2017) Statistical differences in the white matter tracts in subjects with depression by using different skeletonized voxel-wise analysis approaches and DTI fitting procedures. *Brain Research* **1669**, 131–140.

Borkovec T, Ray WJ and Stober J (1998) Worry: a cognitive phenomenon intimately linked to affective, physiological, and interpersonal behavioral processes. *Cognitive Therapy and Research* **22**, 561–576.

Borkovec TD, and Inz J, (1990) The nature of worry in generalized anxiety disorder: A predominance of thought activity. *Behaviour Research and Therapy* **28**, 153–158.

Borkovec TD, Alcaine O and Behar E (2004) Avoidance theory of worry and generalized anxiety disorder. In Heimberg RG, Turk CL and Mennin DS (eds), *Generalized Anxiety Disorder: Advances in Research and Practice*, New York: Guilford Press, pp. 77–108.

Brazier JE, Yang Y, Tsuchiya A and Rowen DL (2010) A review of studies mapping (or cross walking) non-preference based measures of health to generic preference-based measures. *The European Journal of Health Economics* **11**, 215–225.

Brosschot JF, Gerin W and Thayer JF (2006) The perseverative cognition hypothesis: a review of worry, prolonged stress-related physiological activation, and health. *Journal of Psychosomatic Research* **60**, 113–124.

Brown TA, Antony MM and Barlow DH (1992) Psychometric properties of the Penn State Worry Questionnaire in a clinical anxiety disorders sample. *Behaviour Research and Therapy* **30**, 33–37.

Carballedo A, Amico F, Ugwu I, Fagan A, Fahey C, Morris D, Meaney J, Leemans A and Frodl T (2012) Reduced fractional anisotropy in the uncinate fasciculus in patients with major depression carrying the met-allele of

https://doi.org/10.1017/S0033291718002763 Published online by Cambridge University Press

the Val66Met brain-derived neurotrophic factor genotype. *American Journal of Medical Genetics Part B: Neuropsychiatric Genetics* **159**, 537–548.

Chelminski I and Zimmerman M (2003) Pathological worry in depressed and anxious patients. *Journal of Anxiety Disorders* **17**, 533–546.

Cui Z and Gong G (2018) The effect of machine learning regression algorithms and sample size on individualized behavioral prediction with functional connectivity features. *NeuroImage* **178**, 622–637.

Cui Z, Zhong S, Xu P, Gong G and He Y (2013) PANDA: a pipeline toolbox for analyzing brain diffusion images. *Frontiers in Human Neuroscience* **7**, 42.

Cui Z, Su M, Li L, Shu H, Gong G, (2018) Individualized prediction of reading comprehension ability using gray matter volume. *Cerebral Cortex* **28**, 1656–1672.

Cui Z, Xia Z, Su M, Shu H and Gong G (2016) Disrupted white matter connectivity underlying developmental dyslexia: a machine learning approach. *Human Brain Mapping* **37**, 1443–1458.

Dai ZJ, Yan CG, Wang ZQ, Wang JH, Xia MR, Li KC and He Y (2012) Discriminative analysis of early Alzheimer's disease using multi-modal imaging and multi-level characterization with multi-classifier (M3). *NeuroImage* **59**, 2187–2195.

Dalgleish T (2004) The emotional brain. *Nature Reviews Neuroscience* **5**, 583–589.

Damoiseaux JS and Greicius MD (2009) Greater than the sum of its parts: a review of studies combining structural connectivity and resting-state functional connectivity. *Brain Structure and Function* **213**, 525–533.

Dubois J and Adolphs R (2016) Building a science of individual differences from fMRI. *Trends in Cognitive Sciences* **20**, 425–443.

Ecker C, Marquand A, Mourao-Miranda J, Johnston P, Daly EM, Brammer MJ, Maltezos S, Murphy CM, Robertson D, Williams SC and Murphy DG (2010) Describing the brain in autism in five dimensions – magnetic resonance imaging-assisted diagnosis of autism spectrum disorder using a multiparameter classification approach. *Journal of Neuroscience* **30**, 10612–10623.

Ehring T and Watkins ER (2008) Repetitive negative thinking as a transdiagnostic process. *International Journal of Cognitive Therapy* **1**, 192–205.

Erus G, Battapady H, Satterthwaite TD, Hakonarson H, Gur RE, Davatzikos C and Gur RC (2015) Imaging patterns of brain development and their relationship to cognition. *Cerebral Cortex* **25**, 1676–1684.

Etkin A, Prater KE, Schatzberg AF, Menon V and Greicius MD (2009) Disrupted amygdalar subregion functional connectivity and evidence of a compensatory network in generalized anxiety disorder. *Archives of General Psychiatry* **66**, 1361–1372.

Etkin A, Prater KE, Hoeft F, Menon V and Schatzberg AF (2010) Failure of anterior cingulate activation and connectivity with the amygdala during implicit regulation of emotional processing in generalized anxiety disorder. *American Journal of Psychiatry* **167**, 545–554.

Fayers PM and Hays RD (2014) Should linking replace regression when mapping from profile-based measures to preference-based measures? *Value in Health* **17**, 261–265.

Fonzo GA and Etkin A (2017) Affective neuroimaging in generalized anxiety disorder: an integrated review. *Dialogues in Clinical Neuroscience* **19**, 169–179.

Franke K, Ziegler G, Klöppel S, Gaser C and Initiative ASDN (2010) Estimating the age of healthy subjects from T1-weighted MRI scans using kernel methods: exploring the influence of various parameters. *Neuroimage* **50**, 883–892.

Gabrieli JD, Ghosh SS and Whitfield-Gabrieli S (2015) Prediction as a humanitarian and pragmatic contribution from human cognitive neuroscience. *NEURON* **85**, 11–26.

Garibotto V, Scifo P, Gorini A, Alonso CR, Brambati S, Bellodi L and Perani D (2010) Disorganization of anatomical connectivity in obsessive compulsive disorder: a multi-parameter diffusion tensor imaging study in a subpopulation of patients. *Neurobiology of Disease* **37**, 468–476.

Ghashghaei H, Hilgetag C and Barbas H (2007) Sequence of information processing for emotions based on the anatomic dialogue between prefrontal cortex and amygdala. *Neuroimage* **34**, 905–923.

Goh S, Bansal R, Xu D, Hao X, Liu J and Peterson BS (2011) Neuroanatomical correlates of intellectual ability across the life span. *Developmental Cognitive Neuroscience* **1**, 305–312.

Gong Q, Li L, Du M, Pettersson-Yeo W, Crossley N, Yang X, Li J, Huang X and Mechelli A (2014) Quantitative prediction of individual psychopathology in trauma survivors using resting-state FMRI. *Neuropsychopharmacology* **39**, 681–687.

Hermesdorf M, Berger K, Szentkirályi A, Schwindt W, Dannlowski U and Wersching H (2017) Reduced fractional anisotropy in patients with major depressive disorder and associations with vascular stiffness. *NeuroImage: Clinical* **14**, 151–155.

Herrero M-T, Barcia C and Navarro J (2002) Functional anatomy of thalamus and basal ganglia. *Child's Nervous System* **18**, 386–404.

Hettema JM, Kettenmann B, Ahluwalia V, McCarthy C, Kates WR, Schmitt JE, Silberg JL, Neale MC, Kendler KS and Fatouros P (2012) Pilot multimodal twin imaging study of generalized anxiety disorder. *Depression and Anxiety* **29**, 202–209.

Hilbert K, Lueken U and Beesdo-Baum K (2014) Neural structures, functioning and connectivity in generalized anxiety disorder and interaction with neuroendocrine systems: a systematic review. *Journal of Affective Disorders* **158**, 114–126.

Hilbert K, Pine DS, Muehlhan M, Lueken U, Steudte-Schmiedgen S and Beesdo-Baum K (2015) Gray and white matter volume abnormalities in generalized anxiety disorder by categorical and dimensional characterization. *Psychiatry Research: Neuroimaging* **234**, 314–320.

Hoehn-Saric R, Schlund MW and Wong SH (2004) Effects of citalopram on worry and brain activation in patients with generalized anxiety disorder. *Psychiatry Research: Neuroimaging* **131**, 11–21.

Hoehn-Saric R, Lee JS, McLeod DR and Wong DF (2005) Effect of worry on regional cerebral blood flow in nonanxious subjects. *Psychiatry Research: Neuroimaging* **140**, 259–269.

Hoogenboom WS, Perlis RH, Smoller JW, Zeng-Treitler Q, Gainer VS, Murphy SN, Churchill SE, Kohane IS, Shenton ME and Iosifescu DV (2014) Limbic system white matter microstructure and long-term treatment outcome in major depressive disorder: a diffusion tensor imaging study using legacy data. *The World Journal of Biological Psychiatry* **15**, 122–134.

Huang H, Fan X, Williamson DE and Rao U (2011) White matter changes in healthy adolescents at familial risk for unipolar depression: a diffusion tensor imaging study. *Neuropsychopharmacology* **36**, 684–691.

Huys QJ, Maia TV and Paulus MP (2016) Computational psychiatry: from mechanistic insights to the development of new treatments. *Biological Psychiatry: Cognitive Neuroscience and Neuroimaging* **1**, 382–385.

Jenkinson M, Beckmann CF, Behrens TE, Woolrich MW and Smith SM (2012) Fsl. *Neuroimage* **62**, 782–790.

Kazlouski D, Rollin MD, Tregellas J, Shott ME, Jappe LM, Hagman JO, Pryor T, Yang TT and Frank GK (2011) Altered fimbria-fornix white matter integrity in anorexia nervosa predicts harm avoidance. *Psychiatry Research: Neuroimaging* **192**, 109–116.

Khong E, Odenwald N, Hashim E and Cusimano MD (2016) Diffusion tensor imaging findings in post-concussion syndrome patients after mild traumatic brain injury: a systematic review. *Frontiers in Neurology* **7**, 156.

Kim MJ and Whalen PJ (2009) The structural integrity of an amygdala–prefrontal pathway predicts trait anxiety. *Journal of Neuroscience* **29**, 11614–11618.

Kim SJ, Jeong D-U, Sim ME, Bae SC, Chung A, Kim MJ, Chang KH, Ryu J, Renshaw PF and Lyoo IK (2006) Asymmetrically altered integrity of cingulum bundle in posttraumatic stress disorder. *Neuropsychobiology* **54**, 120–125.

Laricchiuta D, Petrosini L, Picerni E, Cutuli D, Iorio M, Chiapponi C, Caltagirone C, Piras F and Spalletta G (2015) The embodied emotion in cerebellum: a neuroimaging study of alexithymia. *Brain Structure and Function* **220**, 2275–2287.

Liao Y, Huang X, Wu Q, Yang C, Kuang W, Du M, Lui S, Yue Q, Chan RC and Kemp GJ (2013) Is depression a disconnection syndrome? Meta-analysis of diffusion tensor imaging studies in patients with MDD. *Journal of Psychiatry & Neuroscience: JPN* **38**, 49–56.

Liao M, Yang F, Zhang Y, He Z, Su L and Li L (2014) White matter abnormalities in adolescents with generalized anxiety disorder: a diffusion tensor imaging study. *BMC Psychiatry* **14**, 41–41.

https://doi.org/10.1017/S0033291718002763 Published online by Cambridge University Press

Makovac E, Meeten F, Watson DR, Herman A, Garfinkel SN, Critchley HD and Ottaviani C (2016) Alterations in amygdala-prefrontal functional connectivity account for excessive worry and autonomic dysregulation in generalized anxiety disorder. *Biological Psychiatry* **80**, 786–795.

Martin AR, Aleksanderek I, Cohen-Adad J, Tarmohamed Z, Tetreault L, Smith N, Cadotte DW, Crawley A, Ginsberg H and Mikulis DJ (2016) Translating state-of-the-art spinal cord MRI techniques to clinical use: a systematic review of clinical studies utilizing DTI, MT, MWF, MRS, and fMRI. *NeuroImage: Clinical* **10**, 192–238.

Martino J, Brogna C, Robles SG, Vergani F and Duffau H (2010) Anatomic dissection of the inferior fronto-occipital fasciculus revisited in the lights of brain stimulation data. *Cortex* **46**, 691–699.

MathWorks (2016) MATLAB documentation. URL: http://www.mathworks.com/access/helpdesk/help/techdoc/.

Meeten F, Davey GC, Makovac E, Watson DR, Garfinkel SN, Critchley HD and Ottaviani C (2016) Goal directed worry rules are associated with distinct patterns of amygdala functional connectivity and vagal modulation during perseverative cognition. *Frontiers in Human Neuroscience* **10**, 553.

Meyer TJ, Miller ML, Metzger RL and Borkovec TD (1990) Development and validation of the penn state worry questionnaire. *Behaviour Research and Therapy* **28**, 487–495.

Modi S, Trivedi R, Singh K, Kumar P, Rathore RK, Tripathi RP and Khushu S (2013) Individual differences in trait anxiety are associated with white matter tract integrity in fornix and uncinate fasciculus: preliminary evidence from a DTI based tractography study. *Behavioural Brain Research* **238**, 188–192.

Mohlman J, Price RB, Eldreth DA, Chazin D, Glover DM and Kates WR (2009) The relation of worry to prefrontal cortex volume in older adults with and without generalized anxiety disorder. *Psychiatry Research: Neuroimaging* **173**, 121–127.

Mori S, Oishi K, Jiang H, Jiang L, Li X, Akhter K, Hua K, Faria AV, Mahmood A and Woods R (2008) Stereotaxic white matter atlas based on diffusion tensor imaging in an ICBM template. *Neuroimage* **40**, 570–582.

Newman MG, Llera SJ, Erickson TM, Przeworski A and Castonguay LG (2013) Worry and generalized anxiety disorder: a review and theoretical synthesis of evidence on nature, etiology, mechanisms, and treatment. *Annual Review of Clinical Psychology* **9**, 275–297.

Paulesu E, Sambugaro E, Torti T, Danelli L, Ferri F, Scialfa G, Sberna M, Ruggiero G, Bottini G and Sassaroli S (2010) Neural correlates of worry in generalized anxiety disorder and in normal controls: a functional MRI study. *Psychological Medicine* **40**, 117–124.

Paulus MP (2015) Pragmatism instead of mechanism: a call for impactful biological psychiatry. *JAMA Psychiatry* **72**, 631–632.

Paulus MP (2017) Evidence-based pragmatic psychiatry – a call to action. *JAMA Psychiatry* **74**, 1185–1186.

Peng H-J, Zheng H-R, Ning Y-P, Zhang Y, Shan B-C, Zhang L, Yang H-C, Liu J, Li Z-X and Zhou J-S (2013) Abnormalities of cortical-limbic-cerebellar white matter networks may contribute to treatment-resistant depression: a diffusion tensor imaging study. *BMC Psychiatry* **13**, 72.

Phan KL, Orlichenko A, Boyd E, Angstadt M, Coccaro EF, Liberzon I and Arfanakis K (2009) Preliminary evidence of white matter abnormality in the uncinate fasciculus in generalized social anxiety disorder. *Biological Psychiatry* **66**, 691–694.

Querstret D and Cropley M (2013) Assessing treatments used to reduce rumination and/or worry: a systematic review. *Clinical Psychology Review* **33**, 996–1009.

Ross A and Jain A (2003) Information fusion in biometrics. *Pattern Recognition Letters* **24**, 2115–2125.

Rowen D, Brazier J and Roberts J (2009) Mapping SF-36 onto the EQ-5D index: how reliable is the relationship? *Health and Quality of Life Outcomes* **7**, 27.

Sarıçiçek A, Zorlu N, Yalın N, Hıdıroğlu C, Çavuşoğlu B, Ceylan D, Ada E, Tunca Z and Özerdem A (2016) Abnormal white matter integrity as a structural endophenotype for bipolar disorder. *Psychological Medicine* **46**, 1547–1558.

Sarubbo S, De Benedictis A, Maldonado IL, Basso G and Duffau H (2013) Frontal terminations for the inferior fronto-occipital fascicle: anatomical dissection, DTI study and functional considerations on a multi-component bundle. *Brain Structure and Function* **218**, 21–37.

Saunders RC and Aggleton JP (2007) Origin and topography of fibers contributing to the fornix in macaque monkeys. *Hippocampus* **17**, 396–411.

Schienle A, Schäfer A, Pignanelli R and Vaitl D (2009) Worry tendencies predict brain activation during aversive imagery. *Neuroscience Letters* **461**, 289–292.

Schutter DJ and Van Honk J (2005) The cerebellum on the rise in human emotion. *The Cerebellum* **4**, 290–294.

Servaas MN, Riese H, Ormel J and Aleman A (2014) The neural correlates of worry in association with individual differences in neuroticism. *Human Brain Mapping* **35**, 4303–4315.

Sharp PB, Miller GA and Heller W (2015) Transdiagnostic dimensions of anxiety: neural mechanisms, executive functions, and new directions. *International Journal of Psychophysiology* **98**, 365–377.

Shen X, Reus L, Adams M, Cox S, Deary I, Liewald D, Bastin M, Smith D, Whalley H and McIntosh A (2017) Subcortical volume and white matter integrity abnormalities in major depressive disorder: findings from UK Biobank imaging data. *Scientific Reports* **7**, 5547.

Sibrava NJ and Borkovec T (2006) The cognitive avoidance theory of worry. In Davey CG and Wells A (eds), *Worry and its Psychological Disorders: Theory, Assessment and Treatment*. West Sussex, England: Wiley & Sons, pp. 239–256.

Smith SM, Jenkinson M, Johansen-Berg H, Rueckert D, Nichols TE, Mackay CE, Watkins KE, Ciccarelli O, Cader MZ, Matthews PM and Behrens TE (2006) Tract-based spatial statistics: voxelwise analysis of multi-subject diffusion data. *Neuroimage* **31**, 1487–1505.

Tipping ME (2001) Sparse Bayesian learning and the relevance vector machine. *Journal of Machine Learning Research* **1**, 211–244.

Tromp DP, Grupe DW, Oathes DJ, McFarlin DR, Hernandez PJ, Kral TR, Lee JE, Adams M, Alexander AL and Nitschke JB (2012) Reduced structural connectivity of a major frontolimbic pathway in generalized anxiety disorder. *Archives of General Psychiatry* **69**, 925–934.

Tseng BY, Gundapuneedi T, Khan M, Diaz-Arrastia R, Levine B, Lu H, Huang H and Zhang R (2013) White matter integrity in physically fit older adults. *Neuroimage* **82**, 510–516.

Versteegh MM, Rowen D, Brazier JE and Stolk EA (2010) Mapping onto Eq-5 D for patients in poor health. *Health and Quality of life Outcomes* **8**, 141.

Wee C-Y, Yap P-T, Li W, Denny K, Browndyke JN, Potter GG, Welsh-Bohmer KA, Wang L and Shen D (2011) Enriched white matter connectivity networks for accurate identification of MCI patients. *Neuroimage* **54**, 1812–1822.

Westlye LT, Bjørnebekk A, Grydeland H, Fjell AM and Walhovd KB (2011) Linking an anxiety-related personality trait to brain white matter microstructure: diffusion tensor imaging and harm avoidance. *Archives of General Psychiatry* **68**, 369–377.

Xie Y, Cui Z, Zhang Z, Sun Y, Sheng C, Li K, Gong G, Han Y and Jia J (2015) Identification of amnestic mild cognitive impairment using multimodal brain features: a combined structural MRI and diffusion tensor imaging study. *Journal of Alzheimer's Disease* **47**, 509–522.

Yarkoni T and Westfall J (2017) Choosing prediction over explanation in psychology: lessons from machine learning. *Perspectives on Psychological Science* **12**, 1100–1122.

Yu S-T, Lee K-S and Lee S-H (2017) Fornix microalterations associated with early trauma in panic disorder. *Journal of Affective Disorders* **220**, 139–146.

Zhang L, Zhang Y, Li L, Li Z, Li W, Ma N, Hou C, Zhang Z, Zhang Z and Wang L (2011) Different white matter abnormalities between the first-episode, treatment-naive patients with posttraumatic stress disorder and generalized anxiety disorder without comorbid conditions. *Journal of Affective Disorders* **133**, 294–299.

Zhang Y, Li L, Yu R, Liu J, Tang J, Tan L, Liao M, Yang F and Shan B (2013a) White matter integrity alterations in first episode, treatment-naive generalized anxiety disorder. *Journal of Affective Disorders* **148**, 196–201.

Zhang Y, Liao M, Tang J, Yang F, Liao Y, Shan B, Liu J and Li L (2013b) White matter microstructure alterations in patients with first episode, treatment-naive generalized anxiety disorder. *Chinese Journal of Psychiatry* **46**, 199–203.

https://doi.org/10.1017/S0033291718002763 Published online by Cambridge University Press